

## ARTICLE



# Effector memory cytotoxic CD3<sup>+</sup>/CD8<sup>+</sup>/CD45RO<sup>+</sup> T cells are predictive of good survival and a lower risk of recurrence in triple-negative breast cancer

Xiangjie Sun<sup>1,6</sup>, Jie Zhai<sup>1,6</sup>, Baohua Sun<sup>1,6</sup>, Edwin Roger Parra<sup>1</sup>, Mei Jiang<sup>1</sup>, Wencai Ma<sup>2</sup>, Jing Wang<sup>2</sup>, Anthony M. Kang<sup>1,3</sup>, Kasthuri Kannan<sup>1</sup>, Renganayaki Pandurengan<sup>1</sup>, Shanyu Zhang<sup>1</sup>, Luisa Maren Solis<sup>1</sup>, Cara L. Haymaker<sup>1</sup>, Maria Gabriela Raso<sup>1</sup>, Julia Mendoza Perez<sup>1</sup>, Aysegul A. Sahin<sup>4</sup>, Ignacio I. Wistuba<sup>1</sup>, Clinton Yam<sup>5</sup>, Jennifer K. Litton<sup>5</sup> and Fei Yang<sup>1</sup>

© The Author(s), under exclusive licence to United States & Canadian Academy of Pathology 2021

Triple-negative breast cancer (TNBC) with high tumour-infiltrating lymphocytes (TILs) has been associated with a promising prognosis. To better understand the prognostic value of immune cell subtypes in TNBC, we characterised TILs and the interaction between tumour cells and immune cell subtypes. A total of 145 breast cancer tissues were stained by multiplex immunofluorescence (mIF), including panel 1 (PD-L1, PD-1, CD3, CD8, CD68 and CK) and panel 2 (Foxp3, Granzyme B, CD45RO, CD3, CD8 and CK). Phenotypes were analysed and quantified by pathologists using InForm software. We found that in the ER-negative (ER <1% and HER2-negative) group and the ER/PR-low positive (ER 1–9% and HER2-negative) group, 11.2% and 7.1% of patients were PD-L1<sup>+</sup> by the tumour cell score, 29.0% and 28.6% were PD-L1<sup>+</sup> by the modified immune cell score and 30.8% and 32.1% were PD-L1<sup>+</sup> by the combined positive score. We combined ER-negative and ER/PR-low positive cases for the survival analysis since a 10% cut-off is often used in clinical practice for therapeutic purposes. The densities of PD-L1<sup>+</sup> tumour cells (HR: 0.366, 95% CI: 0.138–0.970;  $p = 0.043$ ) within the tumour compartment and CD3<sup>+</sup> immune cells in the total area (tumour and stromal compartments combined) (HR: 0.213, 95% CI: 0.070–0.642;  $p = 0.006$ ) were favourable prognostic biomarkers for overall survival (OS) in TNBC. The density of effector/memory cytotoxic T cells (CD3<sup>+</sup>CD8<sup>+</sup>CD45RO<sup>+</sup>) in the tumour compartment was an independent prognostic biomarker for OS (HR: 0.232, 95% CI: 0.086–0.628;  $p = 0.004$ ) and DFS (HR: 0.183, 95% CI: 0.1301–0.744;  $p = 0.009$ ) in TNBC. Interestingly, spatial data suggested that patients with a higher density of PD-L1<sup>+</sup> tumour cells had shorter cell-cell distances from tumour cells to cytotoxic T cells ( $p < 0.01$ ). In conclusion, we found that phenotyping tumour immune cells by mIF is highly informative in understanding the immune microenvironment in TNBC. PD-L1<sup>+</sup> tumour cells, total T cells and effector/memory cytotoxic T cells are promising prognostic biomarkers in TNBC.

*Modern Pathology* (2022) 35:601–608; <https://doi.org/10.1038/s41379-021-00973-w>

## INTRODUCTION

Triple-negative breast cancer (TNBC) is defined by its lack of oestrogen receptor (ER), progesterone receptor (PR) and human epidermal growth factor receptor 2 (HER2) expression. TNBC accounts for 15–20% of all breast cancers worldwide<sup>1,2</sup>. TNBC is diagnosed more frequently in younger women and is more aggressive than other breast cancer subtypes<sup>3,4</sup>. In the past several years, treatment strategies for breast cancer have developed rapidly, and mature systemic therapy, including surgery, chemotherapy, endocrine therapy, radiotherapy and targeted therapy, have substantially improved patient survival<sup>5</sup>. TNBC patients, however, do not benefit from either endocrine therapy or HER2-targeted therapy and have the poorest prognosis<sup>4</sup>.

Immunotherapy, including immune checkpoint inhibitor (ICI) therapy, is an innovative growing area of cancer treatment and has been shown to improve prognosis in melanoma, lung cancer,

head and neck squamous cell carcinoma, urothelial cancer, renal cell cancer and Hodgkin disease<sup>6,7</sup>. In the past 10 years, ICIs and tumour-infiltrating lymphocytes (TILs) have been widely studied, and antibodies against immune checkpoint receptors have been gradually applied to clinical cancer treatment. Therefore, understanding the distribution and prognostic value of TILs in the tumour microenvironment (TME) should expand treatment options for TNBC patients. The TME comprises tumour cells, stromal cells, infiltrating inflammatory cells and vasculature and extracellular matrices, as well as the complex interplay between these cells<sup>8,9</sup>. Successful treatment with ICIs requires the expansion and infiltration of activated lymphocytes into the TME<sup>10</sup>. Therefore, interactions between tumour cells and TILs, along with interactions among TILs, play key roles in cancer immunotherapy.

Immune checkpoints, such as programmed cell death protein 1 (PD-1) and programmed cell death ligand 1 (PD-L1), expressed on

<sup>1</sup>Department of Translational Molecular Pathology, The University of Texas MD Anderson Cancer Center, Houston, TX, USA. <sup>2</sup>Bioinformatics & Computational Biology, The University of Texas MD Anderson Cancer Center, Houston, TX, USA. <sup>3</sup>Department of Computational and Applied Mathematics, Rice University, Houston, TX, USA. <sup>4</sup>Department of Pathology, The University of Texas MD Anderson Cancer Center, Houston, TX, USA. <sup>5</sup>Department of Breast Medical Oncology, The University of Texas MD Anderson Cancer Center, Houston, TX, USA. <sup>6</sup>These authors contributed equally: Xiangjie Sun, Jie Zhai, Baohua Sun. ✉email: [jlitton@mdanderson.org](mailto:jlitton@mdanderson.org); [yangfei72@gmail.com](mailto:yangfei72@gmail.com)

Received: 3 June 2021 Revised: 25 October 2021 Accepted: 4 November 2021

Published online: 27 November 2021

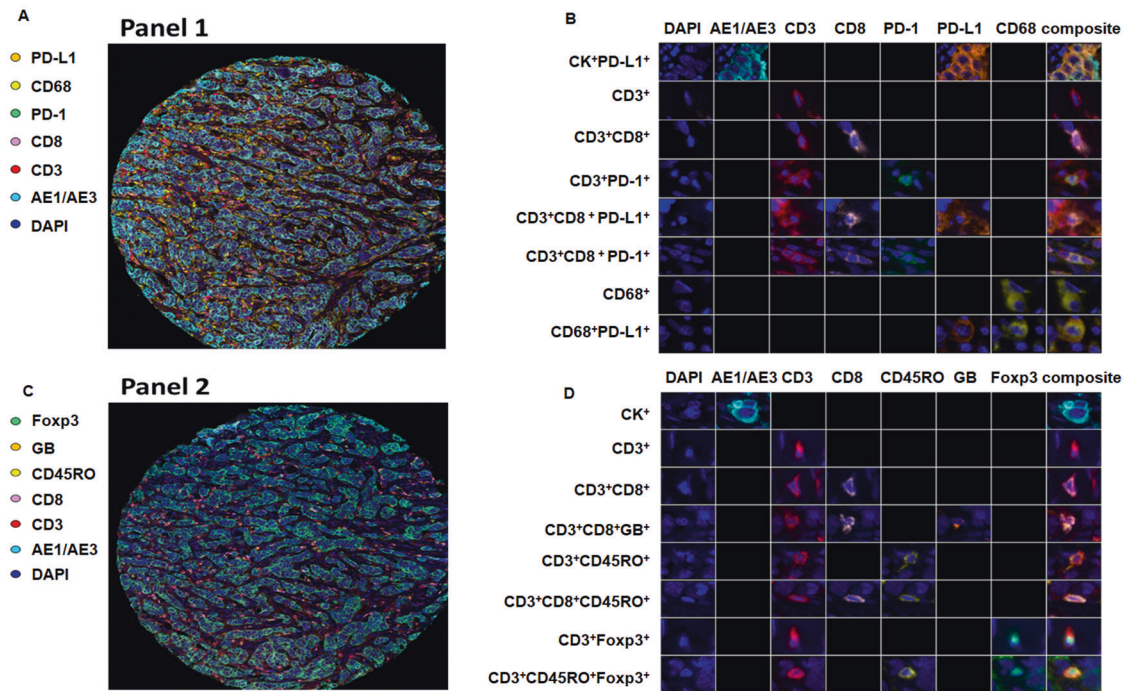


**Fig. 1** Representative mIF images of TNBC cores on FFPE TMA slides. Spectral composite image of TNBC samples stained with **A** panel 1 and **C** panel 2. Individual marker expression in TNBC indicated by immunofluorescence staining with DAPI (blue), cytokeratins (cyan), CD3 (red) and CD8 (pink) in both panels (**B**, **D**); PD-1 (green), PD-L1 (brown) and CD68 (yellow) in panel 1 (**B**); and CD45RO (yellow), granzyme B (GB, brown) and Foxp3 (green) in panel 2 (**D**).

the surface of cancer cells or TILs inhibit T-cell responses by promoting T-cell apoptosis. Therefore, blockade of immune checkpoints could reactivate T-cell responses to kill tumour cells directly. Several ICIs, such as atezolizumab and durvalumab, are being tested in TNBC patients in multiple clinical trials. In the IMpassion130 trial, patients with advanced TNBC with PD-L1<sup>+</sup> TILs in tumour tissue who received atezolizumab plus nab-paclitaxel had better progression-free survival than those who received nab-paclitaxel only<sup>11,12</sup>.

Currently, PD-L1 positivity in both tumour cells and TILs in the TME is determined by immunohistochemical analysis, which makes the simultaneous study of the subpopulation of TILs and PD-L1 difficult. To better understand the impact of PD-L1 expression and TILs on TNBC prognosis, we investigated PD-L1-expressing cells and subtypes of TILs by multiplex immunofluorescence (mIF). mIF can be used to determine the characteristics of the TME by revealing the presence of distinct biomarkers and immunologic phenotypes with less tissue. Chromogenic immunohistochemistry protocols usually only detect one or a small number of markers per slide, and mIF overcomes this limitation by allowing the detection of multiple markers on a single tissue section<sup>13</sup>. In addition, mIF could preserve the spatial context and allow the simultaneous evaluation of multiple immune biomarkers<sup>14,15</sup>. The purpose of our study was to determine the effect of PD-L1 expression and TIL composition on TNBC prognosis.

## MATERIALS AND METHODS

### Tissue samples

We obtained archival formalin-fixed and paraffin-embedded (FFPE) material from breast cancer specimens that had been surgically resected between 2001 and 2013 from the Breast Tumour Bank at The University of Texas MD Anderson Cancer Center (Houston, Texas). The American Society of Clinical Oncology/College of American Pathologists guidelines<sup>16</sup> were used to determine ER, PR and HER2 statuses as part of the routine pathologic evaluation.

Tumour tissue specimens that had been obtained from 145 patients with breast cancer were histologically classified according to the World Health Organization classification of breast tumours and were selected for tissue microarray (TMA) construction. The TMA consisted of 107 breast cancer samples defined as ER-negative (ER/PR <1% and HER2-negative), 28 samples defined as ER/PR-low positive (ER/PR expression in 1–9% of tumour cells and HER2 negativity in all tumour cells)<sup>17</sup> and 10 luminal subtype samples with ER/PR ≥10%. After histologic examination, tumour TMAs were prepared by using triplicate 1-mm-diameter cores per tumour. All cores were taken from the centre of the tumour. Then, 4-µm-thick TMA sections were prepared for mIF staining.

### mIF staining

mIF staining was performed using previously reported validated and optimised methods<sup>18</sup>. In brief, FFPE sections were stained on an automated staining system (BOND-MAX; Leica Microsystems, Buffalo Grove, IL, USA) by using the Opal™ 7-colour Kit (PerkinElmer, Waltham, MA, USA). Normal human tonsil FFPE tissues were also used with and without primary antibodies as positive and negative (autofluorescence) controls, respectively. The markers used for mIF staining were grouped into two panels. Panel 1 consisted of cytokeratin AE1/AE3 (dilution 1:100, Dako, Santa Clara, CA), CD3 (T-cell lymphocytes; polyclonal, dilution 1:200; Dako), CD8 (cytotoxic T cells; clone C8/144B, dilution 1:25; Thermo Fisher Scientific, Waltham, MA, USA), PD-1 (clone EPR4877-2, dilution 1:3000; Abcam, Cambridge, MA, USA), PD-L1 (clone E1L3N, dilution 1:1500; Cell Signaling Technology, Danvers, MA, USA) and CD68 (macrophages; clone PG-M1, dilution 1:50; Dako). Panel 2 consisted of cytokeratin AE1/AE3 (dilution 1:100, Dako), CD3 (T-cell lymphocytes; polyclonal, dilution 1:200; Dako), CD8 (cytotoxic T cells; clone C8/144B, dilution 1:25; Thermo Fisher Scientific), granzyme B (cytotoxic lymphocytes; clone F1, ready to use; Leica Biosystems), Foxp3 (regulatory T cells; clone 206D, dilution 1:50; BioLegend, San Diego, CA, USA) and CD45RO (memory T cells; clone UCHL1, ready to use; Leica Biosystems). The stained slides were scanned by a Vectra multispectral microscope (Vectra 3.0, PerkinElmer). Cell phenotypes (Fig. 1) were identified and counted by trained pathologists using image analysis software (InForm 2.4.8, Akoya Biosciences/PerkinElmer). InForm software offers a user-trainable algorithm for tissue analysis based on morphology and specific markers. To begin the tissue image analysis, the tissue was divided into tumour, stromal and glass compartments using

the tissue segmentation setting by drawing different areas as different categories to train the algorithm. Then, each image was identified as a different tissue compartment. After tissue segmentation, cell segmentation was performed using DAPI for counterstaining to obtain the phenotype of individual cells. We performed cell segmentation using the adaptive cell segmentation setting in InForm software. The splitting parameter was adjusted to segment the crowded and overlapping cells. Membrane or cytoplasmic staining was selected to assist in nuclear segmentation, which is useful for cell identification, especially for multinuclear cells.

After cell segmentation, the algorithm was ready to be trained for cell phenotype identification using a phenotyping setting. When the algorithm training was finished, it was applied in a set of cases to carefully verify that it was working properly on our samples. With the use of these approaches, the optical signal from each phenotype in the spectral unmixing image was isolated and quantified. The data were consolidated with the phenopt package (Akoya Biosciences/PerkinElmer) for R software (Version 3.6.2). Each cell phenotype was evaluated as the average number of cell densities (cells/mm<sup>2</sup>) and/or percentage for analysis in the tumour compartment, stromal compartment and total area (tumour and stromal compartments combined). The markers included CK, CD3 and CD8 and are contained in panels 1 and 2. By assessing the correlation of CK, CD3 and CD8 staining between panels 1 and 2, we found a very high concordance of the three markers with *r* values all over 0.81 (Supplementary Fig. S1). The results used in this study from these three repeated markers are all from panel 1.

### PD-L1 evaluation criteria

The PD-L1 positivity of tumour cells (tumour cell (TC) score) was evaluated as the percentage of malignant cells expressing PD-L1 out of the total number of tumour cells. Immune cell density has been recently used as an alternative immune cell score (IC score) for PD-L1 staining<sup>19,20</sup>. In this study, PD-L1 immune cell positivity was defined as a modified immune cell (mIC) score for mIF. The mIC score was evaluated as the percentage of immune cells (lymphocytes and macrophages) expressing PD-L1 out of the total number of immune cells. The combined positive score (CPS) was obtained by dividing the number of PD-L1<sup>+</sup> tumour cells and immune cells by the total number of tumour cells and multiplying by 100. One per cent was used as the cut-off for PD-L1 positivity.

### Spatial analysis

The spatstat R package was used to create a spatial point for both the tumour and stromal portions of each patient core. The patients were grouped according to whether they had high or low levels of two phenotypes: PD-L1<sup>+</sup> and CD3<sup>+</sup>CD45RO<sup>+</sup>. Spatial metrics were computed only for the tumour portions of each patient core by using spatstat methods. Metric values from multiple cores of the same patient were averaged to obtain one value for each patient. A two-sample two-tailed *t* test was used to determine whether differences between two groups were statistically significant. Differences between the PD-L1<sup>+</sup>-high and PD-L1<sup>+</sup>-low groups were tested for panel 1 markers. Differences between the CD3<sup>+</sup>CD45RO<sup>+</sup>-high and CD3<sup>+</sup>CD45RO<sup>+</sup>-low groups were tested for panel 2 markers. Nearest neighbour distances between two groups of cells were determined with use of the nncross function in R. The nncross method in spatstat was used to conduct spatial analyses between cells of two different markers in each tumour core. This method computes the distance from a cell with marker X to the nearest neighbouring cell with a different marker Y. The average distance is then computed among all cells of the desired marker combination in that core. For each cross analysis between two markers, a *t* test between PD-L1<sup>+</sup>-high and -low or CD3<sup>+</sup>CD45RO<sup>+</sup>-high and -low groups was performed. The nearest neighbour distribution function, also known as the G-function, was performed with the spatstat R package. Typically, the G-function is used to quantify the infiltration of cells of one type into another<sup>21</sup>. In our study, G-function was computed for each tumour core for a single cell phenotype. The G-function was cut off at 50 microns. Then, the area under the curve (AUC) for the G-function of each core was computed. The AUC of the G-function was represented as a measure of clustering: a larger AUC value corresponded to greater clustering.

### Statistical analysis

Categorical variables were compared by the Pearson  $\chi^2$  test, whereas continuous variables were compared by the independent-samples *t* test. Survival analysis was evaluated by the log-rank test and Cox proportional hazards regression. Correlations between different immune cell

populations were assessed using Pearson correlations. An alpha level of 0.05 was used to test for statistical significance. All analyses were performed with SPSS Statistics 24 software (IBM, Armonk, NY).

## RESULTS

### Clinicopathologic features

In the present study, we assessed 145 HER2-negative breast cancer samples, including 107 ER-negative samples (73.8%), 28 ER/PR-low positive samples (19.3%) and 10 luminal subtype samples (6.9%). The clinicopathologic features of this cohort are shown in Table 1. The median age at diagnosis was 53, 50 and 59 years for the ER-negative, ER/PR-low positive and luminal groups, respectively. The most common race for each group was white, followed by black, Hispanic and Asian. Histologic grade III was diagnosed in 81.3% of patients in the ER-negative group and in 92.9% of patients in the ER/PR-low positive group but in only 10% of patients in the luminal subtype group. According to the eighth edition of the American Joint Committee on Cancer staging system, most patients in the ER-negative and ER/PR-low positive groups were categorised as TNM stage II (45.8% and 50%, respectively), followed by stage I (39.2% and 42.9%), stage III (13.1% and 7.1%) and stage IV (1.9% and 0%). In contrast, 50% of patients in the luminal group were categorised as stage I, followed by stage III (30%), stage II (10%) and stage IV (10%).

There were 25.2%, 25% and 20% of patients in the ER-negative, ER/PR-low positive and luminal groups, respectively, who received

**Table 1.** Clinicopathologic features of patients in this cohort.

Parameters	ER-negative		ER/PR-low positive		Luminal	
	(n = 107)		(n = 28)		(n = 10)	
Median age (range) (years)	53	(26–80)	50	(34–83)	59	(36–83)
Race, n (%)						
White	70	(65.4%)	17	(60.7%)	8	(80.0%)
Black	19	(17.8%)	5	(17.9%)	1	(10.0%)
Asian	6	(5.6%)	1	(3.6%)	1	(10.0%)
Hispanic	10	(9.4%)	4	(14.3%)	0	(0%)
Unknown	2	(1.9%)	1	(3.6%)	0	(0%)
Grade, n (%)						
I–II	20	(18.7%)	2	(7.1%)	9	(90.0%)
III	87	(81.3%)	26	(92.9%)	1	(10.0%)
TNM stage, n (%)						
I	42	(39.2%)	12	(42.9%)	5	(50.0%)
II	49	(45.8%)	14	(50.0%)	1	(10.0%)
III	14	(13.1%)	2	(7.1%)	3	(30.0%)
IV	2	(1.9%)	0	(0%)	1	(10.0%)
Neoadjuvant, n (%)						
Yes	27	(25.2%)	7	(25.0%)	2	(20.0%)
No	80	(74.8%)	21	(75.0%)	8	(80.0%)
Adjuvant, n (%)						
Yes	97	(90.7%)	25	(89.3%)	9	(90.0%)
No	10	(9.4%)	3	(10.7%)	1	(10.0%)
Recurrence status, n (%)						
Yes	21	(19.6%)	6	(21.4%)	1	(10.0%)
No	86	(80.4%)	22	(78.6%)	9	(90.0%)

ER/PR oestrogen receptor/progesterone receptor, TNM tumour, node, metastasis.

neoadjuvant therapy; 90.7%, 89.3% and 90.0% of patients in these three groups were treated with adjuvant therapy after surgery. None of the patients received immunotherapy. Strategies of adjuvant therapy included chemotherapy, radiotherapy and endocrine therapy, or their combination, according to molecular subtypes and individual treatment.

After a median follow-up period of 58.2 months, 19.6%, 21.4% and 10% of patients in the ER-negative, ER/PR-low positive and luminal groups, respectively, experienced recurrence or metastasis.

### mIF analysis

Based on cell marker colocalization, the phenotypes shown in panels 1 and 2 include malignant cells expressing PD-L1 (CK<sup>+</sup>PD-L1<sup>+</sup>), cytotoxic T lymphocytes (CD3<sup>+</sup>CD8<sup>+</sup>), antigen-experienced T lymphocytes (CD3<sup>+</sup>PD-1<sup>+</sup>), antigen-experienced cytotoxic T lymphocytes (CD3<sup>+</sup>CD8<sup>+</sup>PD-1<sup>+</sup>), cytotoxic T lymphocytes expressing PD-L1<sup>+</sup> (CD3<sup>+</sup>CD8<sup>+</sup>PD-L1<sup>+</sup>), macrophages expressing PD-L1<sup>+</sup> (CD68<sup>+</sup>PD-L1<sup>+</sup>), activated cytotoxic T lymphocytes (CD3<sup>+</sup>CD8<sup>+</sup>GranzymeB<sup>+</sup>), memory T lymphocytes (CD3<sup>+</sup>CD45RO<sup>+</sup>), effector/memory cytotoxic T lymphocytes (CD3<sup>+</sup>CD8<sup>+</sup>CD45RO<sup>+</sup>), regulatory T lymphocytes (CD3<sup>+</sup>Foxp3<sup>+</sup>) and memory/regulatory T lymphocytes (CD3<sup>+</sup>CD45RO<sup>+</sup>Foxp3<sup>+</sup>) (Fig. 1). Among all of the quantified cell types, we did not find a significant correlation between the densities of any cell subtypes and clinicopathologic parameters. The median number of CK<sup>+</sup> malignant cells was 1696 cells/mm<sup>2</sup> in the total area and 3452.6 cells/mm<sup>2</sup> in the tumour compartment. The number of total CD3<sup>+</sup> T cells was the highest of all immune cells. The number of PD-1<sup>+</sup>-positive or PD-L1<sup>+</sup>-positive cells or both positive immune cells was very small. The tumour compartment cell density of CD3<sup>+</sup>PD-L1<sup>+</sup> cells was significantly higher in ER/PR-low positive patients than in ER-negative patients ( $p < 0.05$ ). In addition, the total area cell density of CD3<sup>+</sup>CD8<sup>+</sup>CD45RO<sup>+</sup> cells was significantly higher in ER/PR-low positive patients than in ER-negative patients ( $p < 0.05$ ). Of note, the sample size of the ER/PR-low positive patients was relatively small ( $n = 28$ ); further studies with more ER/PR-low positive patient samples are needed to validate these findings. No significant differences in other cell densities were found among the three groups (Supplementary Fig. S2).

### PD-L1 evaluation

Cell subtypes expressing PD-L1, including PD-L1<sup>+</sup> tumour cells, PD-L1<sup>+</sup> macrophages and PD-L1<sup>+</sup> lymphocytes, were identified by colocalizing PD-L1 with CK, CD68, CD3 and other markers. Defined as above, 11.2% of patients in the ER-negative group and 7.1% of patients in the ER/PR-low positive group were PD-L1<sup>+</sup> by the TC score, 29.0% and 28.6% by the mIC score, and nearly 30.8% and 32.1% by the CPS, respectively. Patients in the luminal group showed no PD-L1 positivity (Table 2). No significant difference in the PD-L1 positivity rate was detected between ER-negative and ER/PR-low positive patients. Moreover, treatment for ER/PR-low positive patients is similar to treatment for ER-negative patients<sup>22</sup>. Hereafter, we excluded luminal samples and combined ER-negative and ER/PR-low positive patients, referred to as the TNBC group. CK<sup>+</sup>PD-L1<sup>+</sup> cell densities ranged from 0 to 132.32 cells/mm<sup>2</sup>, with a median density of 0 cells/mm<sup>2</sup>. The density of PD-L1<sup>+</sup> macrophages ranged from 0 to 91.43 cells/mm<sup>2</sup>, with a median density of 0 cells/mm<sup>2</sup>. Furthermore, the median percentage of PD-L1<sup>+</sup> macrophages accounting for the total macrophages was 0 (range, 0–58.96%). The densities of CD3<sup>+</sup>PD-L1<sup>+</sup> lymphocytes were low, ranging from 0 to 15.63 cells/mm<sup>2</sup>. A total of 23.36% of all CD3<sup>+</sup> lymphocytes were PD-L1<sup>+</sup>.

### Univariate survival analysis

The median cell density was used as the cut-off value to divide the groups. TNBC patients with a higher density of CK<sup>+</sup>PD-L1<sup>+</sup> cells in the total area had better overall survival (OS) ( $p = 0.03$ ). The same trends were shown for the total CD3<sup>+</sup> immune cells. Patients with a higher

**Table 2.** PD-L1 evaluation of TC score, mIC score, and CPS.

	ER-negative		ER/PR-low positive		Luminal	
	(n = 107)		(n = 28)		(n = 10)	
<i>PD-L1+ (≥1%)</i>						
Tumour cells score	12	(11.2%)	2	(7.1%)	0	(0%)
Modified immune cells score	31	(29.0%)	8	(28.6%)	0	(0%)
CPS	33	(30.8%)	9	(32.1%)	0	(0%)

Tumour cells (TC) score: PD-L1<sup>+</sup> tumour cells/total tumour cells.

Modified immune cells (mIC) score: PD-L1<sup>+</sup> immune cells/total immune cells.

Combined positive score (CPS): PD-L1<sup>+</sup> tumour cells and immune cells/total tumour cells.

density of CD3<sup>+</sup> immune cells also had better OS ( $p = 0.0003$ ) than those with a lower density of CD3<sup>+</sup> immune cells (Fig. 2). Moreover, data from the total area showed that patients with higher densities of CD3<sup>+</sup>CD8<sup>+</sup>, CD3<sup>+</sup>CD8<sup>+</sup>PD-L1<sup>+</sup>, CD3<sup>+</sup>PD-1<sup>+</sup>PD-L1<sup>+</sup>, CD3<sup>+</sup>CD8<sup>+</sup>PD-1<sup>+</sup>PD-L1<sup>+</sup>, CD3<sup>+</sup>CD45RO<sup>+</sup>, CD3<sup>+</sup>CD8<sup>+</sup>GB<sup>+</sup>, CD3<sup>+</sup>CD8<sup>+</sup>CD45RO<sup>+</sup> and CD3<sup>+</sup>CD45RO<sup>+</sup>Foxp3<sup>+</sup> immune cells had better OS (Supplementary Table S1).

For PD-L1 evaluation in the total areas of TNBC samples, we found that 14 patient samples were considered PD-L1<sup>+</sup> by the TC score; however, the number of PD-L1<sup>+</sup> cases increased to 39 when the mIC score was used, and this number was 42 when the CPS was used (Table 2).

Similar univariate survival analysis results were found in the tumour compartment and stromal compartment separately. TNBC patients with a higher density of four types of immune cells (CD3<sup>+</sup>CD45RO<sup>+</sup>, CD3<sup>+</sup>CD8<sup>+</sup>GB<sup>+</sup>, CD3<sup>+</sup>CD8<sup>+</sup>CD45RO<sup>+</sup> and CD3<sup>+</sup>CD45RO<sup>+</sup>Foxp3<sup>+</sup>) in any compartment showed significantly better OS. In addition, TNBC patients with a higher density of specific types of cells, including CD3<sup>+</sup>PD-1<sup>+</sup>, CD3<sup>+</sup>CD8<sup>+</sup>PD-L1<sup>+</sup>, CD3<sup>+</sup>PD-1<sup>+</sup>PD-L1<sup>+</sup>, CD3<sup>+</sup>CD8<sup>+</sup>PD-1<sup>+</sup>PD-L1<sup>+</sup> and CD3<sup>+</sup>CD8<sup>+</sup>Foxp3<sup>+</sup> cells, in the tumour compartment showed significantly better OS. Furthermore, patients with higher densities of CD3<sup>+</sup>CD8<sup>+</sup> and CD3<sup>+</sup>Foxp3<sup>+</sup> immune cells in the stromal compartment also had significantly better OS (Supplementary Table S1).

### Multivariate survival analysis

In the total area, the densities of PD-L1<sup>+</sup> tumour cells and total CD3<sup>+</sup>, CD3<sup>+</sup>CD45RO<sup>+</sup> and CD3<sup>+</sup>CD8<sup>+</sup>CD45RO<sup>+</sup> immune cells were independent prognostic biomarkers for OS in TNBC after adjusting for clinicopathologic parameters. In the tumour compartment, the densities of PD-L1<sup>+</sup> tumour cells and CD3<sup>+</sup>CD8<sup>+</sup>CD45RO<sup>+</sup> immune cells were independent prognostic biomarkers for OS. In the stromal compartment, the density of total CD3<sup>+</sup> immune cells was the only independent prognostic biomarker for OS (Table 3). The density of CD3<sup>+</sup>CD8<sup>+</sup>CD45RO<sup>+</sup> immune cells in the tumour compartment can also independently predict prognosis in terms of disease-free survival (DFS) (HR: 0.183, 95% CI: 0.131–0.744;  $p = 0.009$ ).

### Spatial analysis

The boxplot in Fig. 3 shows that the distances from CK<sup>+</sup> cells to CD3<sup>+</sup>CD8<sup>+</sup> cells were significantly shorter in the PD-L1-high group than in the PD-L1-low group ( $p = 4.77e-05$ ); these distances were also significantly shorter in the CD3<sup>+</sup>CD45RO<sup>+</sup>-high group than in the CD3<sup>+</sup>CD45RO<sup>+</sup>-low group ( $p = 2e-07$ ). In addition, the results showed that the distances from CK<sup>+</sup> cells to CD3<sup>+</sup>Foxp3<sup>+</sup> cells were significantly shorter in the CD3<sup>+</sup>CD45RO<sup>+</sup>-high group than in the CD3<sup>+</sup>CD45RO<sup>+</sup>-low group ( $p = 0.00819$ ) (Fig. 3). Finally, we found that CK<sup>+</sup> cells were clustered less closely together in the CD3<sup>+</sup>CD45RO<sup>+</sup>-high group ( $p = 0.00994$ ); this finding was supported by the

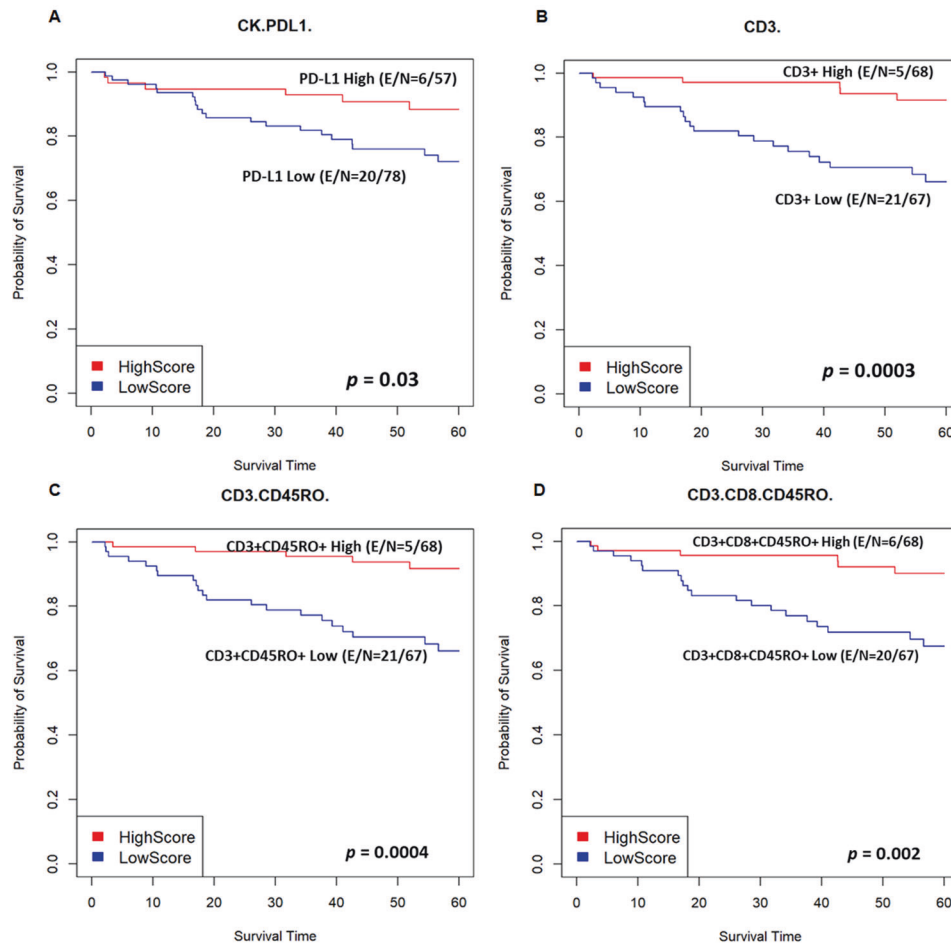


**Fig. 2 Association of PD-L1 expression and effector/memory cytotoxic T cells with survival in TNBC patients.** **A** Kaplan–Meier curves of OS between patients with high and low PD-L1 expression in tumour cells by density in TNBC ( $p = 0.03$ ). **B** Kaplan–Meier curves of OS between patients with high and low densities of T cells in TNBC ( $p = 0.0003$ ). **C** Kaplan–Meier curves of OS between patients with high and low densities of memory T cells in TNBC ( $p = 0.0004$ ). **D** Kaplan–Meier curves of OS between patients with high and low densities of effector/memory cytotoxic T cells in TNBC ( $p = 0.002$ ). *E*, number of patients affected; *N*, number of patients at risk.

G-function AUC analysis. The CK<sup>+</sup> marker yielded significant differences in the AUC between the CD3<sup>+</sup>CD45RO<sup>+</sup>-high and CD3<sup>+</sup>CD45RO<sup>+</sup>-low groups ( $p = 0.00265$ ). The mean AUC was smaller for the CD3<sup>+</sup>CD45RO<sup>+</sup>-high group than for the CD3<sup>+</sup>CD45RO<sup>+</sup>-low group, suggesting that CK<sup>+</sup> cell clustering was sparser in the high group (Fig. 4).

## DISCUSSION

In the present study, we first evaluated the characteristics of PD-L1<sup>+</sup> cells. We then analysed the association between clinical characteristics and prognosis and studied the relationship between TILs and prognosis, as well as the correlations of various TIL phenotypes in the TME of TNBC samples, by using mIF techniques with TMA sections. In addition, we performed spatial analyses of the distance between PD-L1<sup>+</sup> tumour cells and TILs and among various T-cell subtypes, which, to the best of our knowledge, was an innovative exploration.

TILs are generally considered to be the immune cells present in the TME and include cytotoxic T cells, Th cells, dendritic cells, NK cells and macrophages<sup>23,24</sup>. The distribution of TILs in tumour tissues, including TNBC (ER-negative and ER/PR-low positive) tissues<sup>25,26</sup>, is critical for their antitumour or protumour activities. The total area of the tumour tissue includes the tumour compartment and the stromal compartment. We first analysed the phenotypes of TILs in the total area and then

**Table 3.** Multivariate analysis of overall survival (OS).

	Cell types	HR	95% CI	<i>p</i> value
Total area	CK+PD-L1+	0.366	0.138–0.970	0.043
	CD3+	0.213	0.071–0.642	0.006
	CD3+ CD45RO+	0.304	0.109–0.848	0.023
	CD3+CD8+ CD45RO+	0.311	0.112–0.867	0.026
Tumour compartment	CK+PD-L1+	0.366	0.138–0.970	0.043
	CD3+CD8+ CD45RO+	0.232	0.086–0.628	0.004
Stroma compartment	CD3+	0.256	0.092–0.709	0.009

analysed the tumour and stromal compartments separately. In this study, patients with high densities of PD-L1<sup>+</sup> tumour cells had better OS and DFS. Moreover, higher densities of total CD3<sup>+</sup> T cells, CD3<sup>+</sup>CD45RO<sup>+</sup> memory T cells and CD3<sup>+</sup>CD8<sup>+</sup>CD45RO<sup>+</sup> effector/memory cytotoxic T cells predicted better prognosis.

Immune evasion and tolerance are major causes of tumour progression<sup>27</sup>. Recent studies have focused on PD-L1, which plays an important role in maintaining immunosuppression. The most

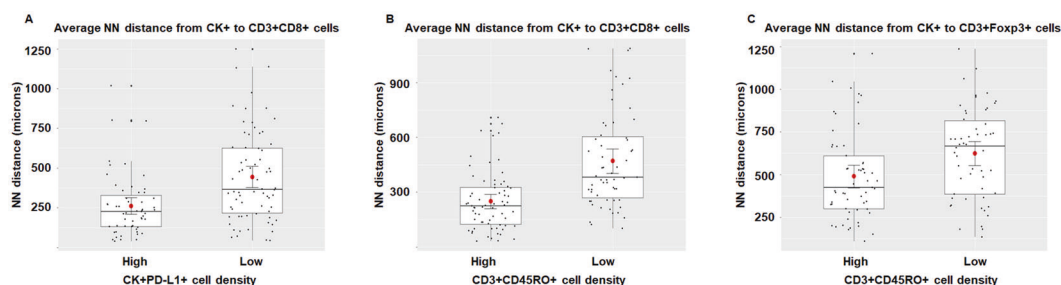


**Fig. 3** Nearest neighbour (NN) distance of tumour cells to TILs in TNBC samples. **A** NN distance of CK<sup>+</sup> cells to cytotoxic T cells in TNBC with high and low PD-L1<sup>+</sup> cell density ( $p = 4.77e-05$ ). **B** NN distance of CK<sup>+</sup> cells to cytotoxic T cells in TNBC with high and low CD3<sup>+</sup>CD45RO<sup>+</sup> cell density ( $p = 2.00e-07$ ). **C** NN distance of CK<sup>+</sup> cells to regulatory T cells in TNBC with high and low CD3<sup>+</sup>CD45RO<sup>+</sup> cell density ( $p = 0.0082$ ).

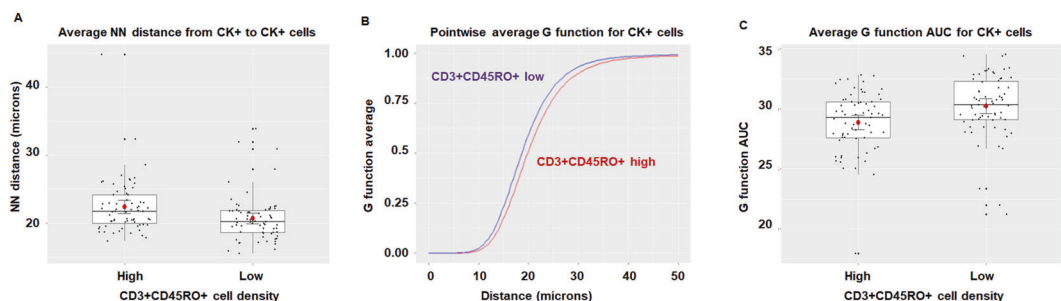


**Fig. 4** Spatial analysis of CK<sup>+</sup> cells. **A** Nearest neighbour (NN) distance of CK<sup>+</sup> cells to CK<sup>+</sup> cells in TNBC samples with high and low CD3<sup>+</sup>CD45RO<sup>+</sup> cell density ( $p = 0.00994$ ). **B** G-function average for CK<sup>+</sup> cells of CD3<sup>+</sup>CD45RO<sup>+</sup>-high and -low samples. **C** G-function AUC distribution corresponding to CK<sup>+</sup> cells between CD3<sup>+</sup>CD45RO<sup>+</sup>-high and -low samples ( $p = 0.00265$ ).

immunogenic subtype of breast cancer is TNBC, which has more TILs in the TME. We also focused on PD-L1 expression in our TNBC samples. Many studies have shown that high PD-L1 expression predicts better survival in TNBC patients<sup>28–31</sup>. The results from these studies, most of which were obtained through immunohistochemical techniques, were consistent with our results. mIF enables the estimation of IC counts at high resolution across numerous high-powered magnification fields and therefore has the potential to produce more accurate and precise estimates of TILs and PD-L1 expression than clinical assays<sup>32</sup>.

Our finding that large quantities of total T cells indicated longer OS in TNBC was consistent with findings from previous studies<sup>33</sup>. No correlation between total T cells and DFS was detected in this study. It is noteworthy that in our results, a high level of total T cells in the total area and the stromal compartment predicted better OS, and no association was found between total T cells in the tumour compartment and prognosis. Based on this finding, we hypothesised that total T cells in the stromal compartment play the main role in antitumour activity. Studies of early-stage TNBC showed that the TIL level in the stromal compartment of TNBC tumours was higher than that in lower-grade tumours and could improve the outcome, which supported our results<sup>34,35</sup>.

Notably, an important finding was that the large numbers of memory T cells in the total area and of effector/memory cytotoxic T cells in both the total area and the tumour compartment were associated with better OS; moreover, the large numbers of effector/memory T cells in the tumour compartment were associated with better DFS in TNBC patients. These findings are consistent with those of previous studies of TNBC and CD8<sup>+</sup> memory T cells<sup>36,37</sup>. In addition, CD8<sup>+</sup> memory T cells expressing GB substantially contributed to TNBC immunosurveillance and are predicted targets for immune checkpoint inhibition<sup>36</sup>. However, no significant correlation was found between CD8<sup>+</sup>-activated memory T cells and prognosis in our results.

In addition to the abundance of lymphocytes, spatial variation has been found to be important for clinical implications<sup>38</sup>. Spatial analysis not only provides additional layers of tumour spatial heterogeneity information but also improves our understanding of the mechanisms behind the formation of the patterns observed in the TME<sup>14,15</sup>. TILs that are close to tumour cells may have a more biologically relevant function than those that are far from the tumour foci<sup>39</sup>. We sought to determine whether various spatial metrics would indicate differences between the PD-L1-high and PD-L1-low groups or between the CD3<sup>+</sup>CD45RO<sup>+</sup>-high and CD3<sup>+</sup>CD45RO<sup>+</sup>-low groups. The nearest neighbour distances between two groups of cells comparing tumour tissue in PD-L1 high versus low patients showed that CK<sup>+</sup> tumour cells are closer to CD3<sup>+</sup>CD8<sup>+</sup> cytotoxic T cells in the PD-L1-high group and the CD3<sup>+</sup>CD45RO<sup>+</sup>-high group. In addition, CK<sup>+</sup> tumour cells were closer to CD3<sup>+</sup>Foxp3<sup>+</sup> regulatory T cells in the CD3<sup>+</sup>CD45RO<sup>+</sup>-high group. The high density of intratumour CD3<sup>+</sup>Foxp3<sup>+</sup> regulatory T cells has been shown to be associated with longer survival in TNBC patients<sup>40</sup>. Further study is needed to better characterise the role of CD3<sup>+</sup>Foxp3<sup>+</sup> regulatory T cells in the treatment of TNBC patients. Moreover, CK<sup>+</sup> tumour cell clustering in CD3<sup>+</sup>CD45RO<sup>+</sup>-high samples was sparser than that in CD3<sup>+</sup>CD45RO<sup>+</sup>-low samples. We also found that CK<sup>+</sup> tumour cells had a negative relationship with CD3<sup>+</sup>CD45RO<sup>+</sup> cells in terms of cell density. It has been reported that high tumour cell density promotes cell migration and metastasis in several tumour models, including TNBC<sup>41</sup>. It remains to be determined whether CD3<sup>+</sup>CD45RO<sup>+</sup> cell density has any correlation with tumour cell migration and metastasis in TNBC.

There are several limitations in the study. First, a limited number of ER/PR-low positive and luminal subtype breast cancer samples were included. Therefore, the comparison of TIL characteristics among different subtypes was not adequate. Second, for the PD-L1 antibody, we chose clone E1L3N based on the previous mIF optimisation rather than one of the currently used clones in the clinic, e.g., SP142, SP263 or 22C3<sup>42</sup>. The variations in the PD-L1

assay by antibody epitope, staining platform and detection system potentially led to different staining sensitivities. Further study may help to answer these concerns about whether the assessments can be used interchangeably.

## REFERENCES

- Bray, F. et al. Global cancer statistics 2018: GLOBOCAN estimates of incidence and mortality worldwide for 36 cancers in 185 countries. *CA Cancer J. Clin.* **68**, 394–424 (2018).
- Siegel, R. L., Miller, K. D. & Jemal, A. Cancer statistics, 2019. *CA Cancer J. Clin.* **69**, 7–34 (2019).
- Bramati, A. et al. Efficacy of biological agents in metastatic triple-negative breast cancer. *Cancer Treat. Rev.* **40**, 605–613 (2014).
- Carey, L. A. et al. Race, breast cancer subtypes, and survival in the Carolina Breast Cancer Study. *JAMA* **295**, 2492–2502 (2006).
- Waks, A. G. & Winer, E. P. Breast cancer treatment: a review. *JAMA* **321**, 288–300 (2019).
- Kruger, S. et al. Advances in cancer immunotherapy 2019 – latest trends. *J. Exp. Clin. Cancer Res.* **38**, 268 (2019).
- Wang, X. et al. Immunological therapy: a novel thriving area for triple-negative breast cancer treatment. *Cancer Lett.* **442**, 409–428 (2019).
- Klemm, F. & Joyce, J. A. Microenvironmental regulation of therapeutic response in cancer. *Trends Cell. Biol.* **25**, 198–213 (2015).
- Devaud, C., John, L. B., Westwood, J. A., Darcy, P. K. & Kershaw, M. H. Immune modulation of the tumor microenvironment for enhancing cancer immunotherapy. *Oncoimmunology* **2**, e25961 (2013).
- Tang, H., Qiao, J. & Fu, Y. X. Immunotherapy and tumor microenvironment. *Cancer Lett.* **370**, 85–90 (2016).
- Schmid, P. et al. Atezolizumab plus nab-paclitaxel as first-line treatment for unresectable, locally advanced or metastatic triple-negative breast cancer (IMpassion130): updated efficacy results from a randomised, double-blind, placebo-controlled, phase 3 trial. *Lancet Oncol.* **21**, 44–59 (2020).
- Adams, S. et al. Patient-reported outcomes from the phase III IMpassion130 trial of atezolizumab plus nab-paclitaxel in metastatic triple-negative breast cancer. *Ann. Oncol.* **31**, 582–589 (2020).
- Mori, H. et al. Characterizing the tumor immune microenvironment with tyramide-based multiplex immunofluorescence. *J. Mammary Gland Biol. Neoplasia.* **25**, 417–432 (2020).
- Mi, H. et al. Digital pathology analysis quantifies spatial heterogeneity of CD3, CD4, CD8, CD20, and FoxP3 immune markers in triple-negative breast cancer. *Front. Physiol.* **11**, 583333 (2020).
- Walens, A. et al. Protein-based immune profiles of basal-like vs. luminal breast cancers. *Lab. Invest.* **101**, 785–793 (2021).
- Hammond, M. E. et al. American Society of Clinical Oncology/College of American Pathologists guideline recommendations for immunohistochemical testing of estrogen and progesterone receptors in breast cancer. *Arch. Pathol. Lab. Med.* **134**, 907–922 (2010).
- Dieci, M. V. et al. Impact of estrogen receptor levels on outcome in non-metastatic triple negative breast cancer patients treated with neoadjuvant/ adjuvant chemotherapy. *NPJ Breast Cancer* **7**, 101 (2021).
- Parra, E. R. et al. Validation of multiplex immunofluorescence panels using multispectral microscopy for immune-profiling of formalin-fixed and paraffin-embedded human tumor tissues. *Sci. Rep.* **7**, 13380 (2017).
- Evans, T. et al. Significance of PD- L1 expressing tumor cells in the combined positive score with triple negative breast cancer. *Cancer Res.* **81**, PS4–PS15 (2021).
- Huemer, F. et al. Impact of PD-L1 scores and changes on clinical outcome in rectal cancer patients undergoing neoadjuvant chemoradiotherapy. *J. Clin. Med.* **9**, 2775 (2020).
- Baddeley, A. & Turner, R. spatstat: an R package for analyzing spatial point patterns. *J. Stat. Softw.* **12**, 1–42 (2005).
- Guo, H. et al. Comparison of three scoring methods using the FDA-approved 22C3 immunohistochemistry assay to evaluate PD-L1 expression in breast cancer and their association with clinicopathologic factors. *Breast Cancer Res.* **22**, 69 (2020).
- Fridman, W. H., Pages, F., Sautes-Fridman, C. & Galon, J. The immune contexture in human tumours: impact on clinical outcome. *Nat. Rev. Cancer* **12**, 298–306 (2012).
- Savas, P. et al. Clinical relevance of host immunity in breast cancer: from TILs to the clinic. *Nat. Rev. Clin. Oncol.* **13**, 228–241 (2016).
- Loi, S. et al. Tumor infiltrating lymphocytes are prognostic in triple negative breast cancer and predictive for trastuzumab benefit in early breast cancer: results from the FinHER trial. *Ann. Oncol.* **25**, 1544–1550 (2014).
- Yam, C. et al. Immune phenotype and response to neoadjuvant therapy in triple-negative breast cancer. *Clin. Cancer Res.* **27**, 5365–5375 (2021).
- Hanahan, D. & Weinberg, R. A. Hallmarks of cancer: the next generation. *Cell* **144**, 646–674 (2011).
- Botti, G. et al. Programmed death ligand 1 (PD-L1) tumor expression is associated with a better prognosis and diabetic disease in triple negative breast cancer patients. *Int. J. Mol. Sci.* **18**, 459 (2017).
- Nanda, R. et al. Pembrolizumab in patients with advanced triple-negative breast cancer: phase Ib KEYNOTE-012 study. *J. Clin. Oncol.* **34**, 2460–2467 (2016).
- Gibson, J. Anti-PD-L1 for metastatic triple-negative breast cancer. *Lancet Oncol.* **16**, e264 (2015).
- Loi, S. et al. Prognostic and predictive value of tumor-infiltrating lymphocytes in a phase III randomized adjuvant breast cancer trial in node-positive breast cancer comparing the addition of docetaxel to doxorubicin with doxorubicin-based chemotherapy: BIG 02-98. *J. Clin. Oncol.* **31**, 860–867 (2013).
- Sanchez, K. et al. Multiplex immunofluorescence to measure dynamic changes in tumor-infiltrating lymphocytes and PD-L1 in early-stage breast cancer. *Breast Cancer Res.* **23**, 2 (2021).
- Yeong, J. et al. Multiplex immunohistochemistry/immunofluorescence (mIHC/IF) for PD-L1 testing in triple-negative breast cancer: a translational assay compared with conventional IHC. *J. Clin. Pathol.* **73**, 557–562 (2020).
- Salgado, R. et al. The evaluation of tumor-infiltrating lymphocytes (TILs) in breast cancer: recommendations by an International TILs Working Group 2014. *Ann. Oncol.* **26**, 259–271 (2015).
- Blackley, E. F. & Loi, S. Targeting immune pathways in breast cancer: review of the prognostic utility of TILs in early stage triple negative breast cancer (TNBC). *Breast* **48**, S44–S48 (2019).
- Savas, P. et al. Single-cell profiling of breast cancer T cells reveals a tissue-resident memory subset associated with improved prognosis. *Nat. Med.* **24**, 986–993 (2018).
- Zhang, S.-C. et al. Clinical implications of tumor-infiltrating immune cells in breast cancer. *J. Cancer* **10**, 6175–6184 (2019).
- Nawaz, S., Heindl, A., Koelble, K. & Yuan, Y. Beyond immune density: critical role of spatial heterogeneity in estrogen receptor-negative breast cancer. *Mod. Pathol.* **28**, 766–777 (2015).
- Dieci, M. V. et al. Update on tumor-infiltrating lymphocytes (TILs) in breast cancer, including recommendations to assess TILs in residual disease after neoadjuvant therapy and in carcinoma in situ: a report of the International Immuno-Oncology Biomarker Working Group on Breast Cancer. *Semin. Cancer Biol.* **52**, 16–25 (2018).
- Yeong, J. et al. Higher densities of Foxp3(+) regulatory T cells are associated with better prognosis in triple-negative breast cancer. *Breast Cancer Res. Treat.* **163**, 21–35 (2017).
- Jayatilaka, H. et al. Tumor cell density regulates matrix metalloproteinases for enhanced migration. *Oncotarget* **9**, 32556–32569 (2018).
- Guo, L., Wei, R., Lin, Y. & Kwok, H. F. Clinical and recent patents applications of PD-1/PD-L1 targeting immunotherapy in cancer treatment-current progress, strategy, and future perspective. *Front. Immunol.* **11**, 1508 (2020).

## ACKNOWLEDGEMENTS

We thank the patients and their families for participating in this study. We thank all the members of our regulatory, clinical, data coordination and translational research teams at the Department of Translational Molecular Pathology, Department of Pathology and Department of Breast Medical Oncology of the MD Anderson Cancer Center for their support on this project. We thank Tamara Locke at the Research Medical Library of the MD Anderson Cancer Center for editing this manuscript.

## AUTHOR CONTRIBUTIONS

F.Y., J.K.L. and I.I.W. made significant contributions to the conceptualisation and project design; X.S., J.Z. and B.S. performed the pathologic analysis and interpretation and the writing and revision of the paper; E.R.P., L.M.S. and M.J. performed the staining and provided technical support; A.A.S. and F.Y. provided tissue material; W.M., J.W., A.M.K., K.K., R.P. and S.Z. performed statistical analysis and spatial analysis; C.L.H., M.G.R., J.M.P. and C.Y. reviewed the data and revised and reviewed the manuscript. All authors read and approved the final paper.

## FUNDING

The study was supported by the Shirley and David Toomim Family Foundation Fund.

## COMPETING INTERESTS

The authors declare no competing interests.

### **ETHICS APPROVAL AND CONSENT TO PARTICIPATE**

This retrospective study was approved by the Institutional Review Board of The University of Texas MD Anderson Cancer Center. This study reviewed data collected from patients as part of routine standard of care; no diagnostic or therapeutic interventions were performed, and no patient contact was involved.

### **ADDITIONAL INFORMATION**

**Supplementary information** The online version contains supplementary material available at <https://doi.org/10.1038/s41379-021-00973-w>.

**Correspondence** and requests for materials should be addressed to Jennifer K. Litton or Fei Yang.

**Reprints and permission information** is available at <http://www.nature.com/reprints>

**Publisher's note** Springer Nature remains neutral with regard to jurisdictional claims in published maps and institutional affiliations.